Electronic Supplementary Material (ESI) for ChemComm.

Electronic Supporting Information

A Cobalt Arylphosphonate MOF – Superior Stability, Sorption and Magnetism

Yunus Zorlu,[b] Doğan Erbahar, [c] Ahmet Çetinkaya, [d] Aysun Bulut,[b,e] Turan. S. Erkal, [f] Ozgur Yazaydin, [g] Jens Beckmann,* [g] Gündoğ Yücesan*[a]

1. Synthesis of [Co(H_4-MTPPA)]·3 NMP·H_2O (1)

Methane-p-tetraphenylphosphonic acid (MTPPA) (0.100 g, 0.35 mmol), $CoSO_4$·7 H_2O (0.150 g, 0.60 mmol), and N-Methyl-2-pyrrolidone (NMP) (9ml) were mixed and this solution was maintained in closed PTFE vessel for 24 hour at 165°C under autogenous pressure. After cooling to room temperature, the dark blue block-shaped crystals were filtered, purified by hand picking under the microscope, washed with acetone, and air-dried with less than ca. 5% yield.

2. X-ray data collection and structure refinement details for 1

Data were obtained with Bruker APEX II QUAZAR three-circle diffractometer. Indexing was performed using APEX2.[S1] Data integration and reduction were carried out with SAINT.[S2] Absorption correction was performed by multi-scan method implemented in SADABS.[S3] The structure was solved using SHELXT[S4] and then refined by full-matrix least-squares refinements on F^2 using the SHELXL[S5] in OLEX[S6] All non-hydrogen atoms were refined anisotropically using all reflections with $I > 2\sigma(I)$. Aromatic and aliphatic C-bound H atoms were positioned geometrically and refined using a riding mode. The P–OH hydrogen atoms were idealized and refined using rigid group (AFIX 147 option of the SHELXL program[S5]). The H atoms of water molecules were located in a difference Fourier map and their positions were constrained to refine on their parent O atoms with Uiso(H) = 1.5Ueq(O). Crystallographic data and refinement details of the data collection for ***1*** are given in Table S1. The selected bond lengths and bond angles are given in Table S2. Crystal structure validations and geometrical calculations were performed using Platon software and mercury was used for visualization of the cif file.[S7-S9] Additional crystallographic data with CCDC reference number 1569569 have been deposited within the Cambridge Crystallographic Data Center *via* www.ccdc.cam.ac.uk/deposit

Table S1. Crystal data and structure refinement details for **1**.

	1
CCDC	1569569
Chemical Formula	$C_{25}H_{20}Co_2O_{12}P_4 \cdot 3(C_5H_9NO) \cdot H_2O$
Formula weight (g. mol^{-1})	1069.56
Temperature (K)	293(2)
Wavelength (Å)	0.71073
Crystal system, Space Group	Monoclinic, $P2_1/n$
a (Å)	12.776(2)
b (Å)	16.835(3)
c (Å)	19.684(3)
α(°)	90
β(°)	90.849(8)
γ(°)	90
Crystal size (mm)	0.08 x 0.09 x 0.20
V (Å^3)	4233.3(13)
Z	4
ρ_{calcd} (g. cm^{-3})	1.678
μ (mm^{-1})	1.014
F(000)	2208
θ range for data collection (°)	2.42 to 22.32
h/k/l	-15<=h<=15, -20<=k<=20, -23<=l<=23
Reflections collected	89104
Independent reflections	7431 [R(int) = 0.196]
Data/restraints/parameters	7431/13/596
Goodness-of-fit on F^2	1.04
R[$F^2 > 2\sigma(F^2)$], wR(F^2)	0.084, 0.243
Largest diff. peak and hole (e.Å^{-3})	1.25 and -0.77

Table S2. Selected bond lengths (Å) and bond angles (°) for the complex **1**.

Bond lengths (Å)					
Co1-O4	1.897 (5)	Co1-O2^{iii}	1.920 (5)	Co1-O7^{i}	1.908 (6)
Co1-O10^{ii}	1.908 (5)	Co2-O3^{ii}	1.909 (5)	Co2-O6	1.893 (6)
Co2-O8^{i}	1.925 (5)	Co2-O12^{iv}	1.898 (5)		
Bond angles (°)					
O4-Co1-O7^{i}	110.2 (3)	O4-Co1-O10^{ii}	103.1 (2)	O7^{i}-Co1-O10^{ii}	115.1 (2)
O4-Co1-O2^{iii}	109.0 (2)	O7^{i}-Co1-O2^{iii}	109.3 (2)	O10^{ii}-Co1-O2^{iii}	109.8 (2)
O6-Co2-O12^{iv}	102.7 (2)	O6-Co2-O3^{ii}	113.2 (2)	O12^{iv}-Co2-O3^{ii}	108.2 (3)
O6-Co2-O8^{i}	112.5 (3)	O12^{iv}-Co2-O8^{i}	109.9 (3)	O3^{ii}-Co2-O8^{i}	110.0 (2)

Symmetry codes: (i) x+1, y, z; (ii) −x+1, −y+1, −z+1; (iii) x+1/2, −y+1/2, z−1/2; (iv) x+1/2, −y+3/2, z−1/2;

Tau(4)-Descriptor for 4-Coordination[S10]

Tau(4) = (360 - (Beta + Alpha)) / 141 = 0.89 :: (Extreme Forms: 0.00 for SQP and 1.00 for TET; 0.85 for TRP)

Tau(4)-Descriptor for 4-Coordination[S10]

Tau(4) = (360 - (Beta + Alpha)) / 141 = 0.93 :: (Extreme Forms: 0.00 for SQP and 1.00 for TET; 0.85 for TRP)

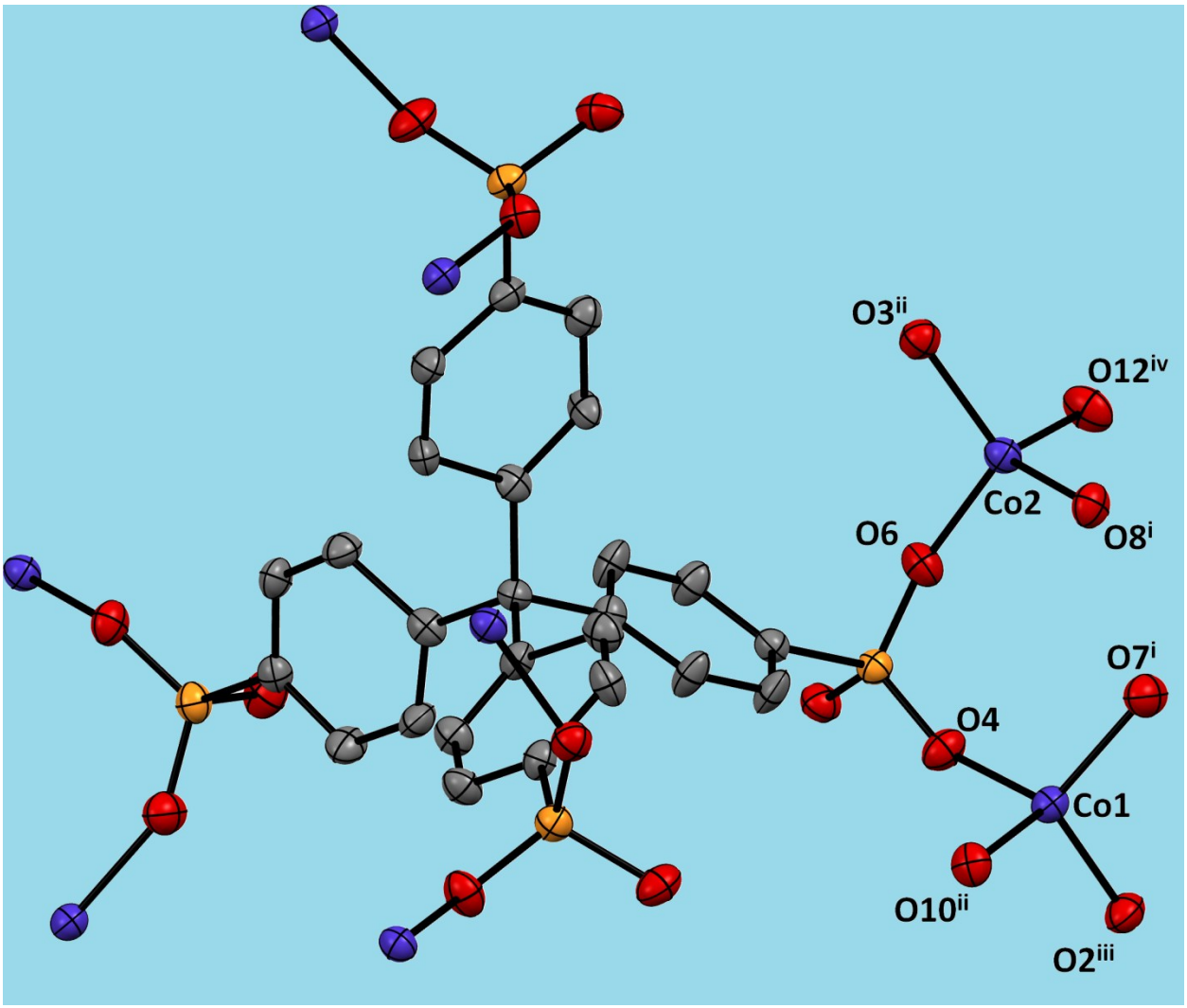

Figure S1. Coordination environment of Co(II) atom in **1**. Displacement ellipsoids are drawn at the 30% probability level. The H-atoms, water molecule, and NMP molecules were omitted for clarity. Symmetry codes: (i) x+1, y, z; (ii) −x+1, −y+1, −z+1; (iii) x+1/2, −y+1/2, z−1/2; (iv) x+1/2, −y+3/2, z−1/2;

3. Thermal stability of 1

SII Nanotechnology – SII6000 Exstar TG/DTA 6300 is used to collect the thermal decomposition pattern of **1**.

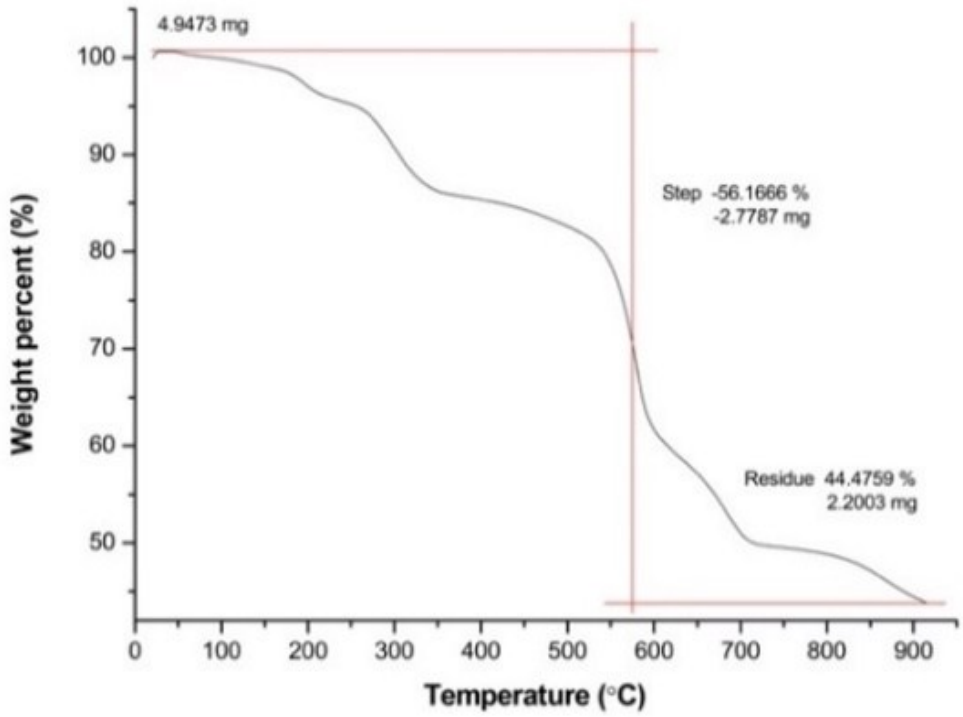

Figure S2. TGA graph of **1**.

4. Molecular simulations.

Classical (force field based) atomistic simulations were performed in order to compute helium porosity and N_2 isotherms in [Co(H_4-MTPPA)]·3 NMP·H_2O. For the simulations we used the RASPA molecular simulations package.[S11] [Co(H_4-MTPPA)]·3 NMP·H_2O unit cell was replicated by 2 × 2 × 2 in the x, y and z directions, respectively, in order to create the simulation cell. Framework atoms were held fixed in their crystallographically determined positions. Interaction energies between non-bonded atoms were computed through the Lennard-Jones (LJ) and Coulomb potentials:

$$V_{ij} = 4\varepsilon_{ij}\left[\left(\frac{\sigma_{ij}}{r_{ij}}\right)^{12} - \left(\frac{\sigma_{ij}}{r_{ij}}\right)^{6}\right] + \frac{q_i\, q_j}{4\,\varepsilon_0\, r_{ij}}$$

where *i* and *j* are interacting atoms, and r_{ij} is the distance between atoms *i* and *j*. ε_{ij} and σ_{ij} are the LJ well depth and diameter, respectively. q_i and q_j are the partial charges of the interacting atoms, and ε_0 is the dielectric constant. In all classical simulations LJ parameters between different types of sites were calculated using the Lorentz-Berthelot mixing rules and the Ewald sum method was employed to compute the electrostatic interactions. LJ interactions were shifted to be 0 at a cutoff distance of 12.0 Å. For the real part of the Ewald summation the cutoff was also 12.0 Å. LJ parameters for the atoms of Co_2H_4-MTPPA (**1**) were taken from the DREIDING[S12] force field except for the cobalt atom; its parameters were taken from UFF (Table S1).[S13] Partial atomic charges for the framework atoms were obtained with the REPEAT method which employs fitting point charges against the electrostatic potential.[S14] In order to generate the electrostatic potential, periodic plane-wave DFT calculations were performed with the CASTEP 16.1 software [S15] using the PBE functional and ultrasoft pseudopotentials with a 550 eV cutoff.

Table S3. LJ parameters for the framework atoms of [Co(H_4-MTPPA)]·3 NMP·H_2O

Atom type	**σ (Å)**	ε/k_B **(K)**
C	3.473	47.856
O	3.033	48.158
H	2.846	7.649
P	3.695	153.476
Co	2.559	7.045

Accessible pore volumes. Accessible pore volumes were computed with the Widom insertion method using a helium probe. This included the random insertion of a single helium atom for 100,000 times in to the frameworks. Then the specific pore volume, V_p, for each structure was determined by

$$V_p = \frac{1}{m_s}\int e^{-\varphi(r)/kT}\, dr$$

where ϕ is the helium-solid potential energy for a single helium atom, *dr* is a differential volume element, and m_s is the mass of solid adsorbent in the simulation box. The helium model was taken from Hirschfelder et al.,[S16] where σ_{He}= 2.640Å and $\varepsilon/k_{B\ He}$= 10.9 K.

N_2 adsorption isotherms and BET surface areas. Grand canonical Monte Carlo (GCMC) simulations were performed in order to simulate the N_2 adsorption isotherms at 77K and up to 0.4 bar. In the grand canonical ensemble the chemical potential, volume and temperature of the system are fixed; however, the number of molecules fluctuate. The GCMC simulations included a 100,000 cycle initialization and a 100,000 cycle production run. Each cycle is n steps, where n is equal to the number of molecules in the system. Random insertions, deletions, translations, rotations and reinsertions of the N_2 molecules were sampled with equal probability. N_2 molecules were modelled using the TraPPE force field,[S17] which was originally fit to reproduce the vapor-liquid coexistence curve of nitrogen.

In this force field the N_2 molecule is a rigid structure where the N-N bond length is fixed at its experimental value of 1.10 Å. This model reproduces the experimental gas-phase quadrupole moment of nitrogen molecule by placing partial charges on nitrogen atoms and on a point located at the center of mass (COM) of the molecule. Table S2 shows the LJ parameters and partial charges for nitrogen.

Table S2. LJ parameters and partial charges for the sites in the N_2 molecule

	σ (Å)	ε/k_B **(K)**	**q (e)**
N	3.31	36.0	-0.482
N_2 COM	0	0	0.964

GCMC simulations report the absolute adsorption data which are then used to compute the excess adsorption data for comparison with experimental data using the relation

$$N_{total} = N_{excess} + \rho_{gas} \times V_p$$

where ρ_{gas} is the bulk density of the gas at simulation conditions which were calculated using the Peng-Robinson equation of state. The BET surface area was obtained by using the simulated N_2 adsorption isotherm of [Co(H_4-MTPPA)]·3 NMP·H_2O and plotting the linear region for the BET equation (Figure S3). The BET surface area is shown in Figure S4. When applying the BET theory, we made sure that our analysis satisfied the two consistency criteria as detailed by Walton et al.[S18]

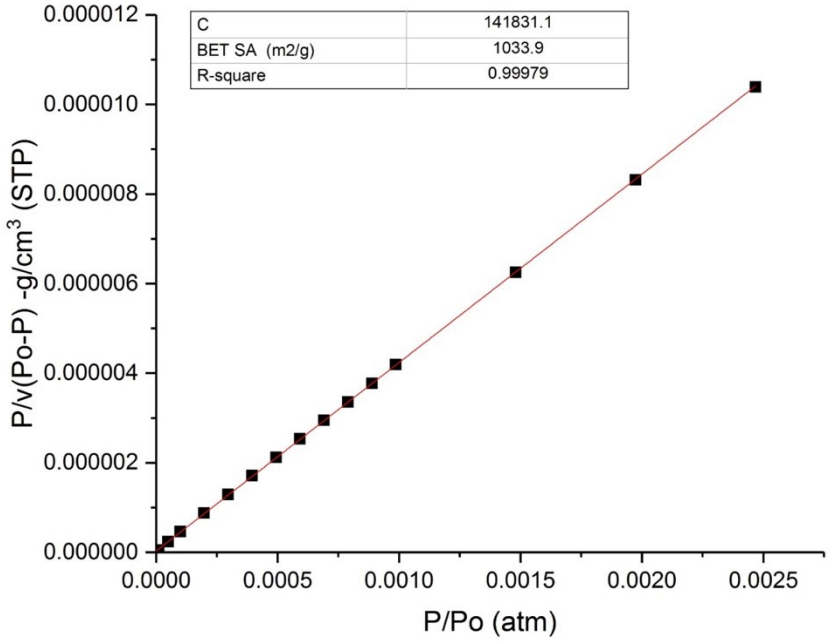

Figure S3. Plot of the linear region for the BET equation.

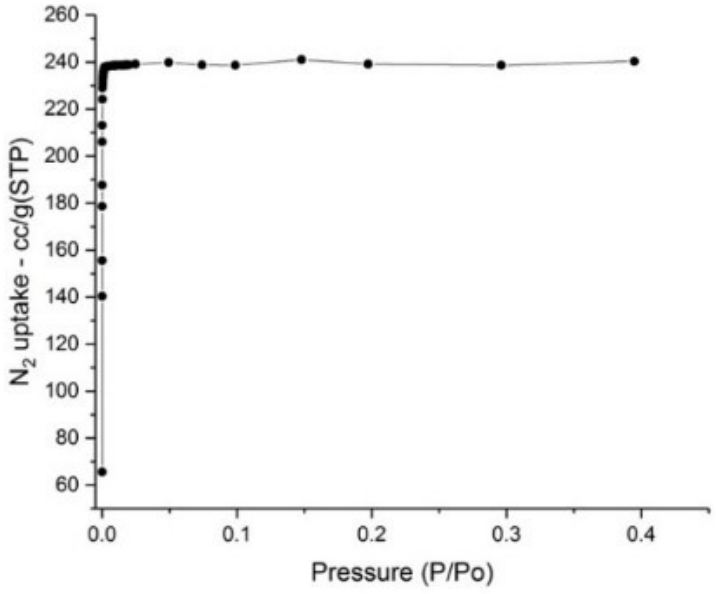

Figure *S*4. Simulated N_2 isotherm of **1** at 77 K.

5. Ab Initio Calculations

Spin polarized density functional theory analysis is performed on the structure that is revealed from XRD data and Electronic structure calculations have been carried out in the framework of density functional theory [S19, S20] within the general gradient approximation (GGA) as implemented in the SIESTA code. [S21, S22] We used Perdew-Burke-Ernzerhof parametrization[S23] for the exchange-correlation functional, and a double-ζ basis set augmented by polarization orbitals. The interaction between the core and valence electrons is handled by Troullier-Martins norm-conserving pseudopotentials[S24] in their fully separable form [S25]. Charge density and potentials are determined on a real-space mesh that corresponds to the plane wave cut-off energy of 200 Ry. The calculations have been spin polarized, charge densities for both spins have been calculated and the difference has been taken to demonstrate the spatial distribution.

6. Additional References

[S1] APEX2, version 2014.11-0, Bruker (2014), Bruker AXS Inc., Madison, WI.

[S2] SAINT, version 8.34A, Bruker (2013), Bruker AXS Inc., Madison, WI.

[S3] SADABS, version2014/5, Bruker (2014), Bruker AXS Inc., Madison, WI.

[S4] G. M. Sheldrick, *Acta Cryst.*, **2015**, *A71*, 3-8.

[S5] G. M. Sheldrick, *Acta Cryst.*, **2015**, *C71*, 3-8.

[S6] O.V. Dolomanov, L.J. Bourhis, R.J. Gildea, J.A.K. Howard, H. Puschmann, J. Appl. Cryst., 2009, 42, 339-341.

[S7] A. L. Spek, *Acta Cryst.* **2009**, *D65*, 148-155.

[S8] A. L. Spek, *Acta Cryst.* **2015**, *C71*, 9-18.

[S9] C. F. Macrae, P. R. Edgington, P. McCabe, E. Pidcock, G. P. Shields, R. Taylor, M. Towler, J. Streek, *J. Appl. Cryst.* **2006**, *39*, 453-457.

[S10] L. Yang, D. R. Powell, R. P. Houser, *Dalton Trans.* **2007**, *0*, 955-964.

[S11] D. Dubbeldam, S. Calero, D. E. Ellis, R. Q. Snurr, *Mol. Sim.* **2016**, *42*, 81-101.

[S12] S. L. Mayo, B. D. Olafson, W. A. Goddard, *J. Phys. Chem*. **1990**, *94*, 8897-8909.

[S13] A. K. Rappe, K. S. Colwell, W. A. Goddard III, W. M. Skiff, *J. Am. Chem. Soc*. **1992**, *114*, 10024-10035.

[S14] C. Campaná, B. Mussard, T. K. Woo, *J. Chem. Theo. Comp*. **2009**, *5*, 2866-2878.

[S15] S. J. Clark, M. D. Segall, C.J. Pickard, P. J. Hasnip, M. J. Probert, K. Refson, M. C. Payne, *Z Kristallogr Cryst Mater* **2005**, *220*, 567-570.

[S16] J. O. Hirschfelder, C. F. Curtiss, R. B. Bird, In Molecular Theory of Gases and Liquids, Wiley: New York, 1954, pp 1114.

[S17] J. J. Potoff, J. I. Siepmann, *AIChE J.* **2001**, *47*, 1676-1682.

[S18] K. S. Walton, R. Q. Snurr, *J. Am. Chem. Soc*. **2007**, *129*, 8552-8556.

[S19] P. Hohenberg and W. Kohn, *Phys. Rev.* 1964, **136**, B864-B871.

[S20] W. Kohn and L. J. Sham, *Phys. Rev.* 1965, **140**, A1133-A1138.

[S21] P. Ordejon, E. Artacho and J. M. Soler, *Phys. Rev. B*, 1996, **53**, 10441-10444.

[S22] J. M. Soler, E. Artacho, J. D. Gale, A. Garcia, J. Junquera, P. Ordejon and D. Sanchez-Portal, *J. Phys. Condensed Matter*, 2002, **14**, 2745-2779.

[S23] J. P. Perdew, K. Burke and M. Ernzerhof, *Phys. Rev. Let.*, 1996, **77**, 3865-3868.

[S24] N. Troullier and J. L. Martins, *Physical Review B*, 1991, **43**, 1993-2006.

[S25] L. Kleinman and D. M. Bylander, *Phys. Rev. Let.* 1982, **48**, 1425-1428.